U = particle migration velocity
$\bar{v}$ = mean fluid velocity
v_{max} = maximum fluid velocity
$\dot{V}$ = total volumetric flow rate through cell
$\dot{V}(a')$ = volumetric flow rate at outlet a′
$\dot{V}(b')$ = volumetric flow rate at outlet b′
$\dot{V}(a)$ = volumetric flow rate at inlet a
$\dot{V}(b)$ = volumetric flow rate at inlet b
$\dot{V}(t)$ = volumetric flow rate of the transport region
V_{ex} = external volume between particles
V_p = pore volume of a particle
V_p^{tot} = total pore volume for all the particles
V_s = volume of the solid part of a particle
V_s^{tot} = total solid volume for all the particles
V_{Sp} = volume of a sphere
V_{tot} = total volume occupied by all particles present in the container
V_{tot}^p = total volume of a particle
w = thickness of the SPLITT channel
$w_{a'}$ = thickness of the fluid lamina between wall A and ISP
w_t = thickness of the transport region
χ_l = magnetic susceptibility of the carrier
χ_p = magnetic susceptibility of a particle
ε = internal porosity
η = suspension viscosity
η_o = carrier viscosity
μ = electrophoretic mobility
ρ_{app} = apparent density
ρ_{bulk} = bulk density
ρ_l = density of the liquid
ρ_s = density of the spherical particle
ω = angular velocity
τ_D = dimensionless diffusion time

See also: **II/Particle Size Separation:** Field Flow Fractionation: Electric Fields; Theory and Instrumentation of Field Flow Fractionation. **III/Polymers:** Field Flow Fractionation.

Further Reading

Allen T (1981) *Particle Size Measurement*, 3rd edn. London: Chapman and Hall.

Contado C, Dondi F, Beckett R and Giddings JC (1997) Separation of particulate environmental samples by SPLITT fractionation using different operating modes. *Analytica Chimica Acta* 345: 99–110.

Contado C, Riello F, Blo G and Dondi F (1999) Continuous split-flow thin cell fractionation of starch particles. *Journal of Chromatography* A 845: 303–316.

Dondi F, Contado C, Blo G and Martin SG (1988) SPLITT cell separation of polydisperse suspended particles of environmental interest. *Chromatographia* 48: 643–654.

Fuh CB and Giddings JC (1995) Isolation of human blood cells, platelets, and plasma proteins by centrifugal SPLITT fractionation. *Biotechnology Progress* 11: 14–20.

Fuh CB and Giddings JC (1997) Separation of submicron pharmaceutic emulsion with centrifugal split-flow thin (SPLITT) fractionation. *Journal of Microseparation* 9: 205–211.

Fuh CB and Chen SY (1998) Magnetic split-flow thin fractionation: new technique for separation of magnetically susceptible particles. *Journal of Chromatography* A 813: 313–324.

Fuh CB, Levin S and Giddings JC (1993) Rapid diffusion coefficient measurements using analytical SPLITT fractionation: application to proteins. *Analytical Biochemistry* 208: 80–87.

Levin S, Myers MN and Giddings JC (1989) Continuous separation of proteins in electrical split-flow thin (SPLITT) cell with equilibrium operation. *Separation Science and Technology* 24(14): 1245–1259.

Provder T (ed.) (1991) *Particle Size Distribution. II. Assessment and Characterization*. ACS Symposium Series 472. Washington DC: American Chemical Society.

Yong J, Kummerow A and Hansen M (1997) Preparative particle separation by continuous SPLITT fractionation. *Journal of Microseparation* 9: 261–273.

Zhang J, Williams PS, Myers MN and Giddings JC (1994) Separation of cells and cell-sized particles by continuous SPLITT fractionation using hydrodynamic lift forces. *Separation Science and Technology* 29(18): 2493–2522.

DropBooks

Theory and Instrumentation of Field Flow Fractionation

J. Janča, Université de la Rochelle, La Rochelle, France

Copyright © 2000 Academic Press

Principle

Field-flow fractionation (FFF) is one of the important analytical methodologies, suitable for the separation and characterization of particles in the submicron and micron ranges. The effective field generates the flux of the separated particles and forms a concentration gradient of each particular species across the ribbon-shaped separation channel. The concentration gradients are counter-balanced by a diffusion flux. At equilibrium, a stable concentration distribution of each particular species is established in the direction across the channel. Simultaneously, a flow velocity profile is formed across the channel due to the viscous

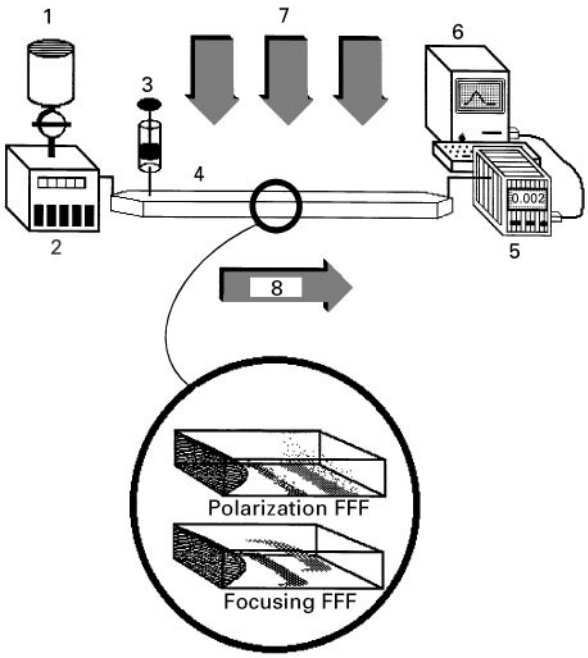

Figure 1 Schematic representation of the general principle and of the experimental arrangement of FFF: (1) carrier liquid reservoir; (2) pump; (3) injector; (4) separation channel; (5) detector; (6) computer; (7) external field; (8) hydrodynamic flow. Detail shows the schematic representation of two fundamental separation mechanisms: polarization FFF and focusing FFF.

drag in the longitudinal flow of the carrier liquid. As a result, each particle is carried along the channel with a velocity corresponding to an instantaneous position of the particle within the flow velocity profile. The carrier liquid thus elutes each species with a mean velocity which corresponds roughly to the position of the centre of gravity of the field-induced concentration distribution across the channel of that species. This principle is schematically demonstrated in **Figure 1**.

The separation is usually governed by the differences in size of the separated components of a polydisperse sample. If the appropriate relationship between the retention parameters and the size of the particles is known or found empirically by using a suitable calibration procedure, the fractograms can be used to calculate the particle size distribution (PSD) and the average values of the particle size of the fractionated species. However, the intensive properties (such as the electrical charge, density, etc.) can influence the separation based on size differences.

Theory of Separation

Two distinguished separation mechanisms, either *polarization* or *focusing*, govern the separation. The separated particles can be differently compressed to the accumulation wall of the channel according to their sizes or focused at different levels across the channel according rather to an intensive property (see Figure 1).

The polarizing field force, F, and the velocity of the field-induced migration of the fractionated particles, U, are usually constant and independent of the position in the direction of the field action:

$$F \neq 0 \text{ and } U \neq 0 \text{ within } 0 < x < w$$

where w is the thickness of the FFF channel in the direction of the field action (x-axis); $x = 0$ is situated at the accumulation wall of the channel. The steady-state concentration distributions of the sample components across the channel are exponential:

$$c_i(x) = c_i(0) \exp\left(-\frac{x}{l_i}\right)$$

where $l_i = D_i/U_i$ is the mean layer thickness, D_i is the diffusion coefficient and c_i is the concentration of the ith species. Larger particles are usually concentrated more closely to the accumulation wall. As a result, the order of the elution is from the small species to larger ones.

The focusing field force and the corresponding velocity U are position dependent:

$$F = f(x), \quad U = f(x) \quad \text{within } 0 < x < w$$
$$F(x) = 0, \quad U(x) = 0 \quad \text{for } x = x_{\max},\ 0 < x_{\max} < w$$

The coordinate $x_{\max}$ corresponds to the position at which the concentration distribution of a focused sample is maximal. Each sample component is focused around its proper $x_{\max}$ position. The steady-state concentration distribution is close to the Gaussian distribution:

$$c(x) = c_{\max} \exp\left[-\frac{1}{2kT}\left(\frac{\mathrm{d}F(x)}{\mathrm{d}x}\right)_{x = x_{\max}} (x - x_{\max})^2\right]$$

where k is the Boltzmann constant and T is the temperature. In some cases the polarization and the focusing mechanisms can act simultaneously.

As mentioned above, a real separation channel is usually ribbon-shaped. However, two parallel infinite planes represent a good approximation of this form. The flow velocity profile established in such a hypothetical channel is parabolic under isoviscous conditions:

$$v(x) = \frac{\Delta P x(x - w)}{2L\mu}$$

where $v(x)$ is the linear velocity of a flow streamline at the position x, ΔP is the pressure drop along the channel of length L, and μ is the viscosity of the carrier liquid.

To describe conveniently the retention of the separated particulate species, the dimensionless retention ratio R is defined:

$$R = \frac{\int_0^w c(x)v(x)\,dx \int_0^w dx}{\int_0^w c(x)\,dx \int_0^w v(x)\,dx}$$

R is the ratio of the average velocity of a retained sample component divided by the average velocity of the carrier liquid. The integration gives the relationship for the polarization FFF

$$R = 6\lambda\left(\coth\left(\frac{1}{2\lambda}\right) - 2\lambda\right)$$

where $\lambda = l/w$. The analogous approximate relationship for the focusing FFF is:

$$R = 6\,(\Gamma_{max} - \Gamma_{max}^2)$$

where $\Gamma_{max} = x_{max}/w$, is the dimensionless coordinate of the maximal concentration of the focused zone. R can be experimentally determined as the ratio of the retention volume (or the retention time) of an unretained sample component (equal to the volume of the channel) divided by the retention volume (retention time) of the retained sample component. The simple and known relationship between the λ and the particle size make it possible to calculate the PSD from the experimental retention data.

Each fractionation is based on transport processes which lead to the formation of the concentration gradients. From the thermodynamic point of view, the general entropic tendency of a closed system is to erase such gradients by molecular motion. As a result, the spreading of the zones due to dispersion processes occurs. The zone spreading can be quantitatively described by the height equivalent to a theoretical plate H:

$$H = L\left(\frac{\sigma}{V_R}\right)^2$$

where V_R is the retention volume and σ is the standard deviation of the zone of uniform size particles. The elution curve (fractogram) of a polydisperse sample thus reflects the contribution of the spreading processes superposed over the fractionation according to the PSD.

In order to calculate a true PSD from the experimental raw fractogram, a correction for the zone spreading should be applied. It is based on the deconvolution of an experimental fractogram $h(V)$ of a polydisperse particulate sample which is a superposition of the true PSD $g(Y)$ and the spreading function $G(V, Y)$ representing the zone of uniform particles having the elution volume Y:

$$h(V) = \int_0^\infty g(Y)G(V, Y)\,dY$$

where V and Y are then the elution volumes. This equation, called the Tung integral equation, is the basis for all well-known correction methods and can be solved analytically under the condition that the spreading function is uniform. In this case, the convolution integral to be solved is:

$$h(V) = \int_0^\infty g(Y)G(V - Y)\,dY$$

In a number of practical cases, the spreading function can be approximated by the normal Gaussian function. The application of the correction of an experimental fractogram is demonstrated in **Figure 2**.

The true PSD can be expressed as a number of the particles of a given diameter n_i relative to the number of all the particles in the sample:

$$N_i = \frac{n_i}{\sum_0^\infty n_i}$$

or as the mass of the particles m_i of a given diameter d_i relative to the total mass of the sample:

$$M_i = \frac{m_i}{\sum_0^\infty m_i}$$

The PSD can be used further to calculate various average particle sizes such as the mass average particle diameter:

$$\bar{d}_m = \frac{\sum_0^\infty m_i d_i}{\sum_0^\infty m_i} = \frac{\sum_0^\infty h_i d_i}{\sum_0^\infty h_i}$$

or the number average particle diameter:

$$\bar{d}_n = \frac{\sum_0^\infty n_i d_i}{\sum_0^\infty n_i} = \frac{\sum_0^\infty h_i}{\sum_0^\infty h_i/d_i}$$

DropBooks

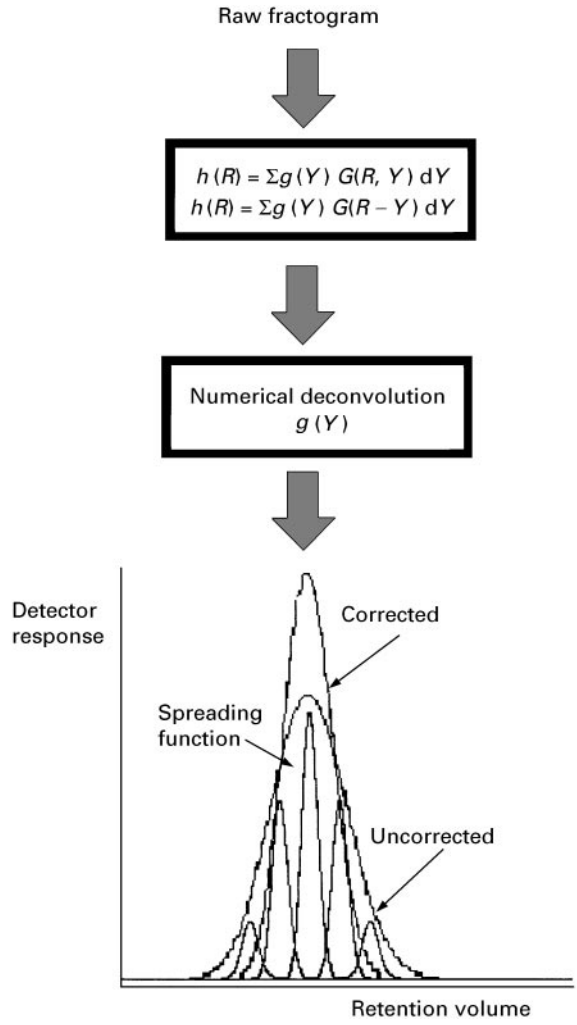

Figure 2 Schematic representation of a procedure for the treatment of a raw experimental fractogram to correct for zone broadening.

where h_i is the normalized detector response to the ith particle diameter. The polydispersity of the fractionated sample can be characterized, for example, by the index of polydispersity:

$$I = \frac{\bar{d}_{\mathrm{m}}}{\bar{d}_{\mathrm{n}}}$$

The above basic theory and data treatment can be applied independently of a particular FFF method or technique.

Instrumentation

Polarization FFF

In particle size separations by FFF, the nature of the applied field (physical or chemical forces) determines each particular method or technique of polarization FFF and, consequently, the appropriate instrumentation. The most important polarization FFF methods at the present time are:

- sedimentation FFF
- flow FFF
- electric FFF
- thermal FFF

The basic experimental devices as well as specific instrumentation are described here for each particular FFF method or technique.

Independent of the method or technique, all FFF apparatuses are composed of a system of solvent delivery (reservoir, pump), injector sample (injection valve, syringe-septum, etc.), separation channel (different construction for each method), detector (refractive index detector, spectrophotometer, molar mass detector, etc.) and a data acquisition and treatment system (computer). With the exception of the FFF separation channel, all other components, and the system as a whole, are practically the same as a conventional liquid chromatography system.

Schematic representation of the separation channel for *sedimentation FFF* is shown in **Figure 3**(A). The separation channel is coiled inside a centrifuge rotor. A delicate part of this separation unit is the rotating seal which must permit the flow-through of a carrier liquid and the connection to the injector at the entry to the channel proper and of a detector at the exit. However, this technical problem is solved and the rotors for sedimentation FFF are commercially available. On the other hand, a home-built solution is also possible providing that some technical skill is available.

If the particles to be separated are relatively large or dense and, consequently, the gravitational force is enough to generate the formation of sufficiently strong concentration gradients, the construction of the separation channel is much simpler, as shown in Figure 3(B). In this case, the channel is composed of two sandwiched glass plates, one of them is provided with holes and capillaries for carrier liquid entry and exit and a thin foil in which the channel proper is cut. The whole channel must be positioned horizontally to avoid casual parasite convections which could cause the separation to deteriorate.

The channel for *flow FFF* is schematically demonstrated in **Figure 4**(A). It is formed between two parallel, semipermeable membranes fixed on porous supports. The cross-flow of the carrier liquid is superposed perpendicularly to the flow of the carrier liquid in a longitudinal direction inside the channel. The cross-flow acts as an external field of hydrodynamic forces which generate a uniform flux of all particles.

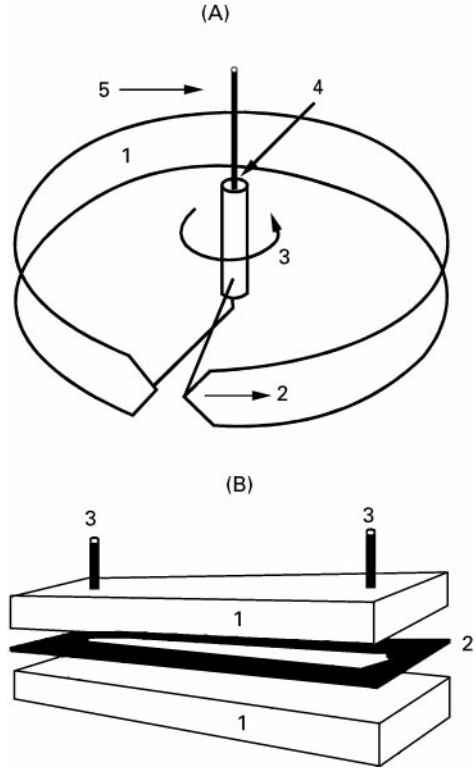

Figure 3 Simplified schemes of the construction of the sedimentation FFF channels used in a centrifuge and in natural gravitational field. (A) Sedimentation FFF channel: (1) channel; (2) direction of the flow; (3) rotation; (4) flow inlet; (5) flow outlet. (B) Gravitational FFF channel: (1) channel walls; (2) foil spacer; (3) inlet and outlet.

The carrier liquid passes through the membranes but the separated particles should not, due to the conveniently chosen porosity of the membranes. The uniformity of the cross-flow is, however, not necessary to achieve high performance separation. If only one of the main channel walls is semi-permeable, a non-uniform hydrodynamic field is generated in such an asymmetrical flow FFF channel. The dependence of the separation resolution on particle size in such a channel is different compared with a channel equipped with two semi-permeable walls, but high performance particle size separation is also achieved.

A classical type of rectangular cross-section channel has sometimes been substituted with a circular cross-section capillary with an overpressure applied inside or by applying an external cross-flow in a more standard manner, as shown in Figure 4(B). The simplicity of the construction of such a 'channel' is the main advantage of this configuration. The theoretical description of the separation is complex, however, and, moreover, the probability of the formation of parasite flows degenerating the separation is higher.

The channel for *electric FFF* is usually formed by semipermeable membranes as in flow FFF (see **Figure 5**). The reason for such a solution is to decouple the separation channel proper from the electrode chambers and thus to avoid the contamination of the channel by products of electrolysis (gas bubbles). However, channels of simpler construction in which the metal or graphite electrodes form the channel walls and thus are not decoupled from the separation space have been constructed and work quite well under carefully chosen experimental conditions. The channel for *thermal FFF* is constructed in such a manner to allow a temperature difference between two metallic bar walls with highly polished surfaces. The walls are separated by a spacer in which the channel proper is cut. The upper bar is heated by using appropriate electrical cartridges and the lower bar is cooled by circulating water. Both bars should be equipped with several holes to accommodate the thermocouples for temperature control. Schematic representation of a channel for thermal FFF is shown in **Figure 6**. In some cases, when the temperature of

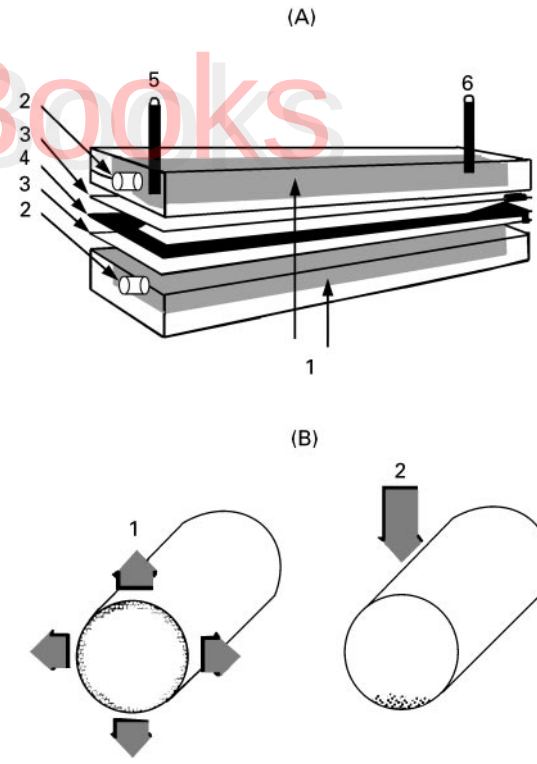

Figure 4 (A) Construction of a rectangular cross-section channel for flow FFF: (1) porous supports; (2) cross-flow inlet and outlet; (3) membranes; (4) foil spacer; (5) longitudinal flow inlet; (6) longitudinal flow outlet. (B) Circular capillary for flow FFF with: (1) overpressure applied from the inside; (2) cross-flow applied externally.

DropBooks

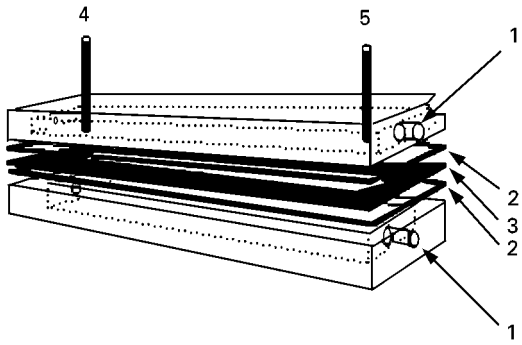

Figure 5 Construction of a channel for electric FFF: (1) electrodes and electrolyte inlet and outlet; (2) membranes; (3) foil spacer; (4) longitudinal flow inlet; (5) longitudinal flow outlet.

the heated wall is above the boiling point of the carrier liquid used, the channel must be sealed so as to operate under high-pressure conditions. The thickness of the channel can be as low as few micrometers which permits performing high-speed and high-resolution fractionations. The separation can be accomplished in just a few seconds.

Focusing FFF

Focusing FFF methods have been classified according to various combinations of the driving field forces and gradients:

- effective property gradient of the carrier liquid,
- cross-flow velocity gradient,
- lift forces,
- shear stress, and
- gradient of the non-homogeneous field action.

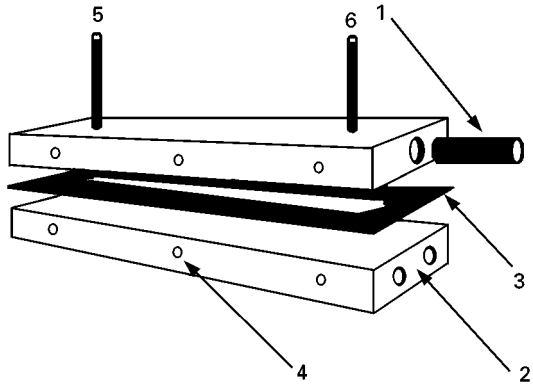

Figure 6 Construction of a channel for thermal FFF: (1) electric heating cartridge; (2) cooling liquid inlet and outlet; (3) foil spacer; (4) holes for thermocouples; (5) longitudinal flow inlet; (6) longitudinal flow outlet.

While this classification scheme is perfectly consistent with fundamental separation mechanisms and related driving forces, particular focusing FFF methods and techniques are more often called according to experimental procedure. The instrumentation will be described for each implemented focusing FFF method or technique.

The channels for sedimentation–flotation focusing field-flow fractionation (SFFFFF) or isoelectric focusing field-flow fractionation (IEFFFF) are either of standard rectangular cross-section or of modulated cross-sectional permeability (for example, of trapezoidal or triangular cross-section), as shown in **Figures 7**(A) and (B). While the flow velocity profile in channels of rectangular cross-section are symmetrical (e.g. parabolic), the modulated cross-sectional permeability channels allow formation of flow velocity profiles which are not symmetrical. The advantage of these channels is that almost all zones focused symmetrically regarding the central longitudinal axis of the separation channel can be separated. If the flow velocity profile is symmetrical, the zones focused at the opposite sides regarding the central axis of the channel can be confused.

Both above-mentioned methods belong to the first category in which an effective property gradient of the carrier liquid represents the major driving force. The focusing in these cases can appear to be due to the effective property gradient of the carrier liquid in the direction across the channel combined with the primary or secondary transverse field.

It has been shown that the gradient of the effective property of the carrier liquid can be performed at the beginning of the channel. For example, the step density gradient can easily be formed by pumping the carrier liquids of various densities through several inlet capillaries into the channel. Such an arrangement can effectively be used for continuous preparative fractionation providing that the separation channel is also equipped with several outlet capillaries to continuously collect the fractions which are focused at different levels. Schematic representation of such a channel is shown in **Figure 8**.

The elutriation focusing field-flow fractionation (EFFFF) method belongs to the category in which the focusing is due to the gradient of transversal flow velocity of the carrier liquid which opposes the action of the external field. The longitudinal flow of the carrier liquid is acting simultaneously. A trapezoidal cross-section as well as a rectangular cross-section channels can be used in this case. Schematic representation of such a channel for elutriation FFF is

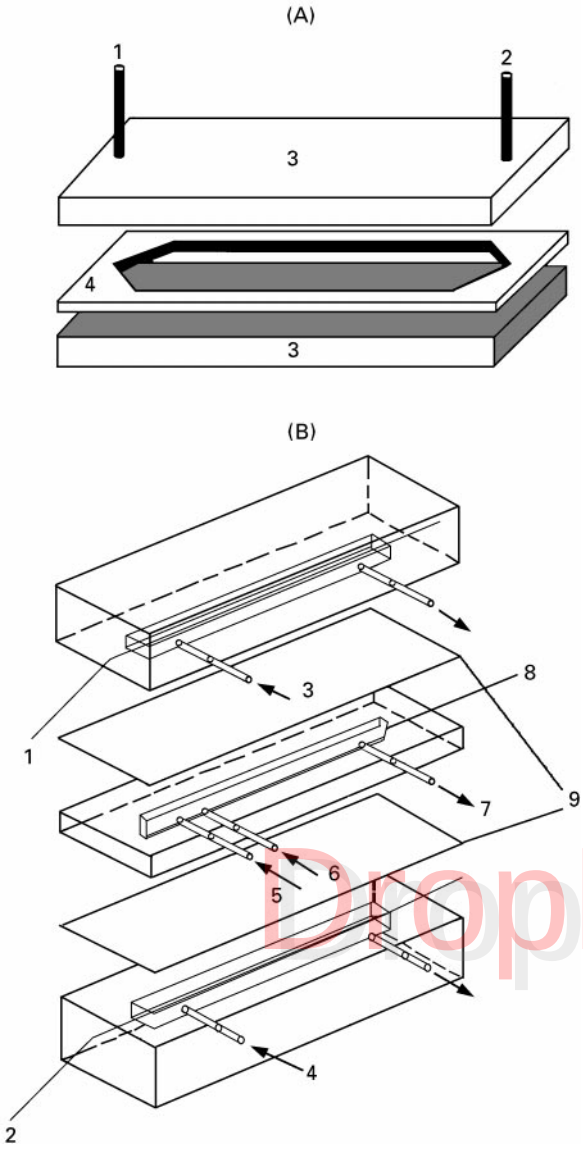

Figure 7 (A) Schematic representation of a channel for sedimentation flotation focusing FFF in coupled electric and gravitational fields: (1) flow in; (2) flow out; (3) electrodes forming the channel walls; (4) spacer. (B) Schematic representation of a trapezoidal cross-section channel for isoelectric focusing FFF: (1) Pt anode; (2) Pt cathode; (3) anolyte; (4) catholyte; (5) ampholyte; (6) sample; (7) to detector; (8) trapezoidal cross-section channel; (9) membranes.

shown in **Figure 9**. The channel shown has a trapezoidal cross-section which causes formation not only of a convenient, axially asymmetrical flow velocity profile but, providing the volumetric transversal flow-in and flow-out are equal, a linear velocity gradient is established across the channel. In combination with different constant velocities of different size-separated particles the conditions for the focusing phenomenon to appear are established.

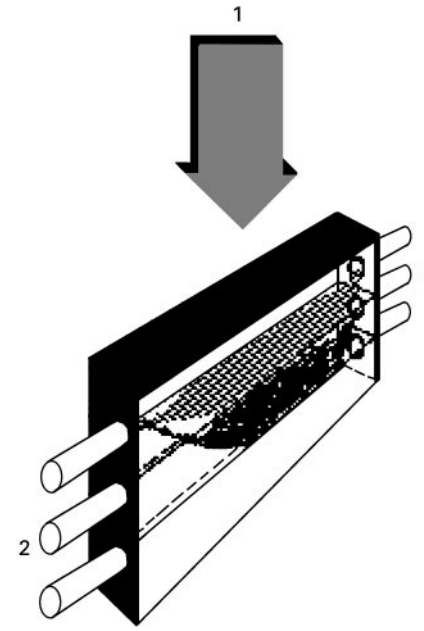

Figure 8 Continuous preparative channel for focusing FFF in preformed step density gradient: (1) gravitational field; (2) flow inlets; (3) flow outlets.

Very few experiments have been published on FFF exploiting the hydrodynamic lift forces at high carrier flow rates which, with the high shear gradient, result in the deformation of soft particles and their subsequent displacement and focusing. Similarly little has been published on FFF using a non-homogeneous high gradient external field. Although these methods can, in principle, use one of the types of channel described above for other focusing FFF methods, no experimental proof for this currently exists.

DropBooks

Conclusion

A large number and variety of homemade channels exist which confirms that in most cases, the construction of a channel is not extremely difficult.

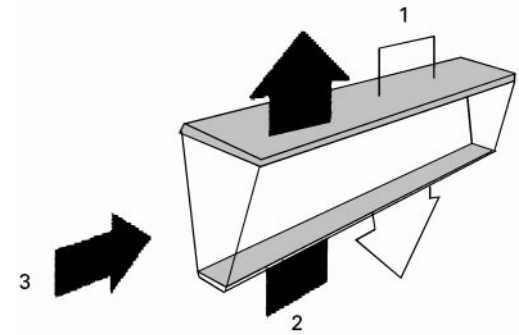

Figure 9 Schematic representation of a channel for elutriation focusing FFF: (1) field force; (2) cross-flow; (3) longitudinal flow.

However, commercial FFF apparatus is increasingly available which could further stimulate interest in applying this high performance separation methodology in routine laboratory practice.

See also: **II/Particle Size Separation:** Field Flow Fractionation: Electric Fields. **III/Cells and Cell Organelles: Field Flow Fractionation.**

Further Reading

Barth HG (ed.) (1984) *Modern Methods of Particle Size Analysis*. New York: John Wiley.

Janča J (1987) *Field-flow fractionation*: *analysis of macromolecules and particles*. New York: Marcel Dekker.

Janča J (1995) Isoperichoric focusing field-flow fractionation based on coupling of primary and secondary field action In: Provder T, Barth HG and Urban MW (eds) *Chromatographic Characterization of Polymers*, *Hyphenated and Multidimensional Techniques*. *Advances in Chemistry Series* 247. Washington DC: American Chemical Society.

Janča J (1999) Field-flow fractionation. In: Pethrick RA and Dawkins JV (eds) *Modern Techniques for Polymer Characterisation*. New York: John Wiley.